View Online / Journal Homepage / Table of Contents for this issue
Dynamic Article Links

Journal of
Materials Chemistry

Cite this: *J. Mater. Chem.*, 2012, **22**, 4599

www.rsc.org/materials

COMMUNICATION

Atomic layer deposition of tin oxide with nitric oxide as an oxidant gas†

Jaeyeong Heo, Sang Bok Kim and Roy G. Gordon*

Received 13th December 2011, Accepted 16th January 2012
DOI: 10.1039/c2jm16557k

Downloaded by Harvard University on 22 February 2012
Published on 03 February 2012 on http://pubs.rsc.org | doi:10.1039/C2JM16557K

Atomic layer deposition (ALD) of tin oxide (SnO_2) thin films was achieved using a cyclic amide of Sn(II) (1,3-bis(1,1-dimethylethyl)-4,5-dimethyl-(4R,5R)-1,3,2-diazastannolidin-2-ylidene) as a tin precursor and nitric oxide (NO) as an oxidant gas. Film properties as a function of growth temperature from 130–250 °C were studied. Highly conducting SnO_2 films were obtained at 200–250 °C with the growth per cycle of ∼1.4 Å/cycle, while insulating films were grown at temperatures lower than 200 °C. Conformal growth of SnO_2 in holes of aspect-ratios up to ∼50 : 1 was successfully demonstrated.

Introduction

Tin oxide (SnO_2) is an n-type semiconductor with wide band gap of ∼3.6 eV that shows high conductivity when doped with fluorine.[1,2] The combination of high transparency, infrared reflectivity, and conductivity has led to applications of SnO_2 such as energy-conserving windows for buildings,[3] gas sensors,[4,5] and transparent electrodes/conductors in thin-film solar cells.[6–8] Recently, there has been a need for making transparent conducting oxides on various nanostructures with high surface areas such as solar cells. High light absorption is enabled by nanostructures, which provides a large surface area to increase the conversion efficiency of the cells.[6–11]

The authors recently reported a successful growth of SnO_2 by atomic layer deposition (ALD) at 60–250 °C by using a newly synthesized cyclic amide of Sn(II) (1,3-bis(1,1-dimethylethyl)-4,5-dimethyl-(4*R*,5*R*)-1,3,2-diazastannolidin-2-ylidene) and 50 wt.% hydrogen peroxide (H_2O_2).[12] The growth per cycle was as high as 1.8 Å/cycle and the lowest resistivity of $\sim 2 \times 10^{-2}$ ohm cm was obtained at a growth temperature of 120 °C. In order to get conformal growth of SnO_2 on structures with high aspect-ratios, the growth temperature needed to be lowered to ∼60 °C to extend the lifetime of H_2O_2 molecules diffusing inside narrow features. The highest conformality of this approach, however, was only ∼80% in a hole with aspect-ratio of ∼50 : 1 (diameter ∼200 nm). Also, it was found that the overexposure of H_2O_2 on growing SnO_2 surface increases the film's resistivity. Given the nonuniform profile of H_2O_2 concentration along the holes due to its decomposition, uniform resistivity along the structure cannot be guaranteed,[12] similar to films grown by plasma-assisted ALD.[13] The usage of thermally sensitive H_2O_2 will be more problematic when SnO_2 should be formed on nm-sized porous features of large surface area, where extremely long exposure time is needed to infiltrate highly torturous template structures.[6,14–18] Therefore, it is important to find an alternative oxidant gas that shows high reactivity toward the Sn(II) precursor without premature decomposition while making films highly conductive and transparent.

In this communication, we report that nitric oxide (NO) can be used as an effective oxidant gas with this Sn(II) precursor. No previous reports have been found for the usage of NO as an oxidant gas for ALD. Nitric oxide shows high reactivity toward the Sn(II) precursor and the growth per cycle was as high as ∼1.4 Å/cycle at 250 °C. Conformal growth of conducting SnO_2 was achieved in holes with aspect ratios up to ∼50 : 1. This ALD SnO_2 process is expected to be widely useful for coating nanostructures with high surface areas and extremely narrow or complex features.

Experimental

SnO_2 thin films were deposited using a custom-built hot-wall ALD reactor. A stop-flow ALD injection scheme where the pulse step is divided into fill and hold was employed to obtain highly conformal SnO_2 films.[19] Detailed operation procedure as well as the information on the Sn(II) precursor can be found in our previous report.[12] The tin precursor was held in a bubbler at 40 °C, which generated a vapor pressure of 0.42 Torr. Nitric oxide (Airgas) was used as an oxidant gas for the Sn(II) precursor. Nitric oxide was first filled into a trap volume (2.1 mL) and subsequently delivered to the reaction chamber, which enables the precise control over the dosage. The pressure of NO in the reaction chamber was set to be ∼2 Torr and hold time was set to be 30s to facilitate its reaction with the Sn precursor and to allow deep penetration into a high-aspect-ratio structure. The purge time after Sn precursor and oxidant pulses was set to be 45s to completely remove unreacted species to prevent reaction in vapor phase. Growth temperature was changed from 130 to 250 °C based on a thermal decomposition result for the Sn precursor (Fig. S1†).

The film thickness, surface roughness, and density were evaluated by using X-ray reflectivity (XRR, PANAlytical, X'Pert Pro) with commercial software (X'Pert Reflectivity ver. 1.1). A single-wavelength ellipsometry (LSE-W, Gaertner Scientific) was used to obtain the refractive index of the films. The electrical resistivity, carrier type, carrier concentration, and mobility were determined by van der Pauw measurements of the Hall effect. The compositions of the films

Department of Chemistry and Chemical Biology, Harvard University, Cambridge, Massachusetts, 02138, USA. E-mail: gordon@chemistry.harvard.edu; Fax: +1-617-495-4723; Tel: +1-617-496-5393

† Electronic Supplementary Information (ESI) available: Growth temperature and optical properties. See DOI: 10.1039/c2jm16557k

Downloaded by Harvard University on 22 February 2012
Published on 03 February 2012 on http://pubs.rsc.org | doi:10.1039/C2JM16557K

deposited on a glassy carbon substrate (Alfa Aesar) were measured by *ex situ* Rutherford backscattering spectroscopy (RBS). The thermal decomposition of the precursor was tested by using X-ray fluorescence (XRF, Spectro, Xepos III). The microstructure of the films was evaluated by glancing-angle X-ray diffraction (GAXRD, ω = 0.4°, PANAlytical, X'Pert Pro) and high-resolution transmission electron microscopy (HRTEM, JEOL, JEM-2100). A TEM grid with a supporting ~50 nm-thick silicon nitride membrane window (Ted Pella) was used as a substrate. Conformality of SnO_2 films on a hole structure of aspect-ratio of ~50 : 1 was tested by using field-emission scanning electron microscopy (FESEM, Zeiss, Ultra 55). Optical properties of the film were measured by a UV-Vis spectrophotometer (Hitachi, U-4100).

Results and discussion

The reactivity between the cyclic Sn(II) precursor and NO was studied as a function of growth temperature and the growth per cycle and refractive index are shown in Fig. 1a. From the growth per cycle curve the growth behavior can be divided mainly into two regions, below and above 230 °C. The growth per cycle is as high as ~2.3 Å/cycle at 130 °C and decreases sharply with increasing growth temperature up to 200 °C. Also, the refractive index in this low-temperature region is much lower (1.77–1.95) than the reported value for ideal SnO_2 (~2),[17] suggesting the growth of low-density films at low temperatures. It appears that although the reaction between the Sn(II) precursor and NO occurs at low growth temperature (<230 °C), the resulting film density is lower than bulk SnO_2. For the films grown at 130 and 170 °C, a longer purge time of 90s was tested to check for a possible CVD reaction, but a similar growth per cycle was obtained. When the growth temperature was increased to 230–250 °C, the bulk refractive index of ~2 is observed with the saturated growth per cycle of ~1.4 Å/cycle. This value of ~2 is even higher than the SnO_2 film (~1.95) grown by the combination of Sn(II) precursor and H_2O_2.[12] When a SnO_2 film was grown at 280 °C, we noted

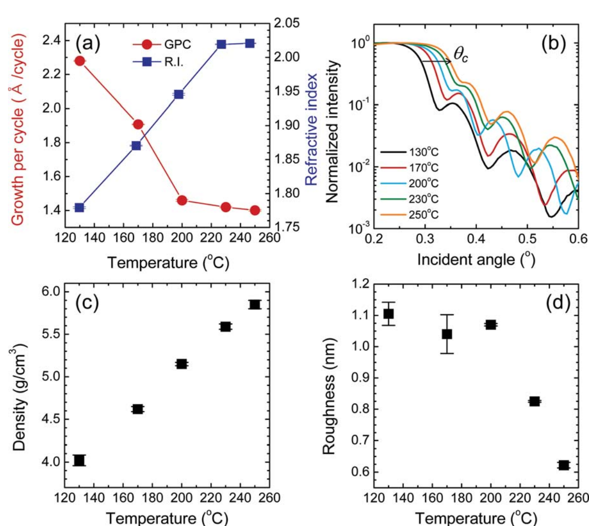

Fig. 1 (a) Growth per cycle and refractive index as a function of growth temperature. (b) Normalized X-ray reflectivity spectra for SnO_2 films grown at 130–250 °C. The critical angle (θ_c) increases with increasing growth temperature. (c) The simulated film densities and (d) surface roughness of the films.

a small increase in refractive index (~2.05), which may be due to some incorporation of a SnO-rich phase (n = 2.4)[17] coming from thermally decomposed Sn atoms (Fig. S1†).

The high reactivity of NO as an oxidant for ALD was suggested by Won *et al.*, who observed complete monolayer growth of ZrO_2 (~1.8 Å/cycle) using a N_2O plasma.[20] The authors claimed that NO groups generated by the N_2O plasma are responsible for the enhanced growth per cycle based on an in-depth X-ray photoelectron spectroscopy study.

The film density was estimated by using XRR analyses on SnO_2 films grown at 130–250 °C on glass substrates. Here, all film thicknesses are 30–35 nm. Fig. 1b shows the normalized reflectivity spectra and it is seen that a critical angle (θ_c), where the intensity of reflected X-ray is at half maximum,[15,21] increases with the growth temperature. This result confirms a gradual increase in film density with the growth temperature. The simulated film densities are summarized in Fig. 1c. When the growth temperature is 130 °C, the film density is ~4.02 g cm^{-3} and it increases up to ~5.85 g cm^{-3} for 250 °C-grown SnO_2. The bulk density of SnO_2 is known to be 6.95–6.99 g cm^{-3} and the highest density of ~5.85 g cm^{-3} corresponds to ~84% of the bulk value.[22] Interestingly, film shrinkage was observed when e-beam was irradiated on the films grown at 130 and 170 °C for SEM analysis, which is consistent with their low film densities. The growth per cycle calculated after film shrinkage of these films was ~1.5 Å/cycle which is close to ~1.4 Å/cycle for the films grown at 200–250 °C. Densification of the growing films is accelerated at higher growth temperature. Lower film roughness was also observed for films grown at higher temperatures (230 and 250 °C) as shown in Fig. 1d.

Electrical properties of SnO_2 films grown at different growth temperatures were accessed by Hall measurements. The plot of Fig. 2a shows that resistivity drastically decreases with increasing growth temperature from 130 to 200 °C. As suggested by refractive index (Fig. 1a) and density (Fig. 1c), high resistivity of the low-temperature films may come from their low density. Then, resistivity slowly drops further at above 200 °C. The film with the highest growth temperature of 250 °C has the lowest resistivity of ~8×10^{-3} ohm cm. The measured mobility and carrier concentration are summarized in Fig. 2b. Due to its high resistivity, the mobility and carrier concentration could not be determined for the film grown at 130 °C. The increase in carrier concentration was responsible for about two orders of magnitude decrease in resistivity from 170 to 200 °C. The carrier concentration of SnO_2 films grown at above 200 °C exhibits a saturated value of ~1–2 × 10^{20} cm^{-3}. The further drop in resistivity from 230 to 250 °C came mainly from the increase in mobility from 2.5 to 6.1 cm^2 V^{-1} s^{-1}.

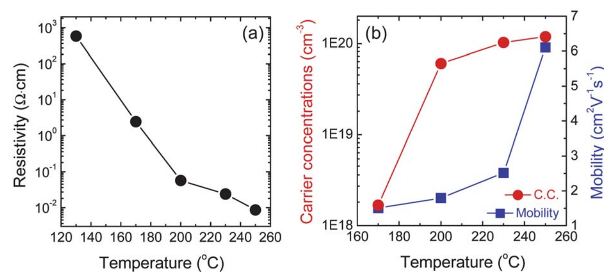

Fig. 2 (a) Electrical resistivity change as a function of growth temperature. (b) Carrier concentration and mobility obtained from the Hall measurements.

 This journal is © The Royal Society of Chemistry 2012

Published on 03 February 2012 on http://pubs.rsc.org | doi:10.1039/C2JM16557K
Downloaded by Harvard University on 22 February 2012

The composition of SnO_2 the films was analyzed by RBS and a representative spectrum for a SnO_2 film grown at 250 °C is shown in Fig. 3a. In addition to tin and oxygen signals from the film, a weak nitrogen signal was also observed. Fig. 3b shows the magnified nitrogen signal of Fig. 3a. Here, a RBS spectrum from the film grown at 130 °C was also shown for reference (gray). The atomic ratio of nitrogen to oxygen was found to decrease from ~9 to ~2.7% as the growth temperature increased from 130 to 250 °C, as shown in Fig. 3c. No carbon was detected in the RBS signal just above carbon in the substrate, although a percent of carbon in the film might not be observable above the ~1% ^{13}C in the substrate. The nitrogen is more likely to come from the NO gas than from the ligand of the precursor, because otherwise a large amount of carbon would accompany the nitrogen. At least for the films grown at high temperature (200–250 °C) it appears that this nitrogen does not trap free carriers based on the high carrier concentrations (~1–2 × 10^{20} cm^{-3}). The O/Sn ratio decreases from 2.13 to 1.93 as the growth temperature increases from 130 to 250 °C, as shown in Fig. 3d. The RBS analysis shows that the film becomes closer to stoichiometric SnO_2 as the growth temperature is increased up to 250 °C.

Fig. 4a shows the cross-sectional SEM images of the SnO_2 film grown at 250 °C on holes of aspect-ratio of ~50 : 1. Completely conformal growth of conducting SnO_2 was achieved. When 50 wt.% H_2O_2 was used, the decomposition of the oxidant led to the limited conformality of SnO_2 on holes with the same structure.[12] From the GAXRD analysis on ~60 nm-thick SnO_2 film grown at 250 °C on a glass substrate as shown in Fig. 4b, slightly crystallized rutile SnO_2 (JCPDS #41-1445) was identified as evidenced by broad peaks centered at ~30 and ~54°. The high resolution plan-view TEM image of Fig. 4c also confirms its nano-crystallinity. Here, the thickness of the films was ~35 nm and the growth temperature was 250 °C. Compared to the SnO_2 film grown at 120 °C by 50 wt.% H_2O_2, a less crystallized SnO_2 film was obtained.[12] This lower crystallinity might be due to the small amount of nitrogen in the film, which may inhibit crystal growth.

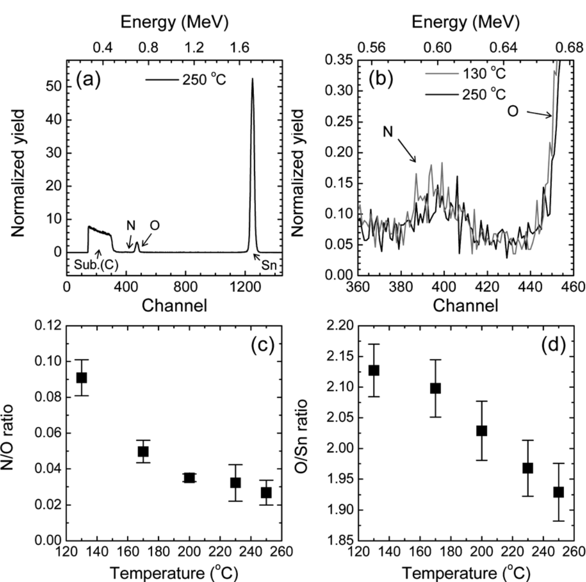

Fig. 3 (a) A representative RBS spectrum for a SnO_2 film grown on a carbon substrate at 250 °C. (b) The magnified spectra of the nitrogen region for SnO_2 films grown at 130 (gray) and 250 (black) °C. (c) The measured N/O and (d) O/Sn ratios. The error bars represent maximum and minimum values from simulations.

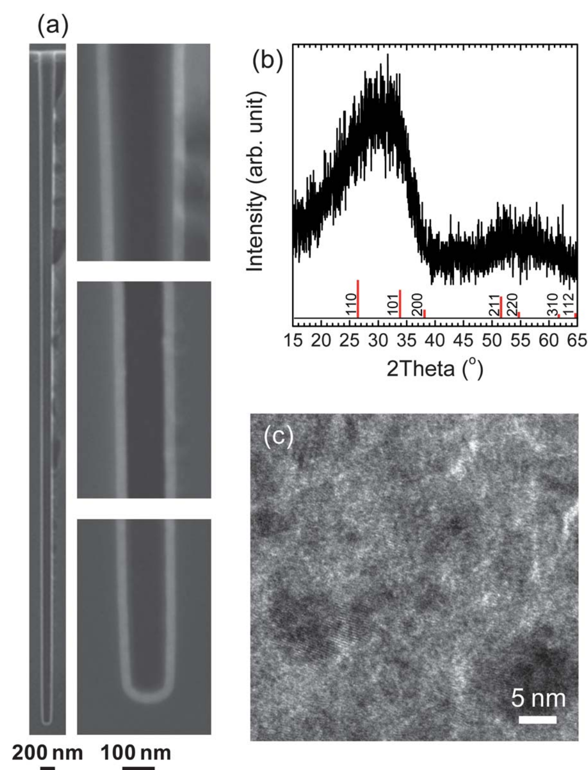

Fig. 4 (a) Cross-sectional SEM image of a hole with aspect ratio ~50 : 1 coated by SnO_2 at 250 °C and magnified views of the top, middle, and bottom of the coated hole. (b) GAXRD spectrum for ~60 nm-thick SnO_2 grown at 250 °C on a glass substrate. The bars at the bottom of the figure present the peak positions of SnO_2 rutile phase with their relative intensities (JCPDS #41-1445). (c) High resolution plan-view TEM image of a SnO_2 film grown on a silicon nitride membrane at 250 °C.

Optical properties of the SnO_2 film grown on a quartz substrate at 250 °C were evaluated (Fig. S2†). The average transmission in the visible region from 400 to 700 nm was 87.2%, which is comparable to other reports for ALD-grown SnO_2.[12,17] The estimated band gap of the SnO_2 film was 4.23–4.27 eV.

Conclusion

In summary, conducting SnO_2 films were formed using a newly synthesized cyclic amide of Sn(II) as a precursor and nitric oxide as an oxidant gas. It was found that growth temperature plays a crucial role on determining film's overall properties. Growth per cycle of ~1.4 Å/cycle was found at growth temperature of 200–250 °C with the lowest resistivity of ~8 × 10^{-3} ohm cm and mobility over 6 cm^2 V^{-1} s^{-1} at 250 °C. The density of the film increased with growth temperature. The SnO_2 films were nano-crystalline. The average transmission for the visible range was as high as 87.2% for a film ~110 nm thick with sheet resistance ~780 ohms per square. Conformal growth of SnO_2 in holes of aspect ratios up to ~50 : 1 was successfully demonstrated.

Acknowledgements

This work was performed in part at the Center for Nanoscale Systems (CNS) at Harvard University, a member of the National

Nanotechnology Infrastructure Network (NNIN), which is supported by the National Science Foundation under NSF award no. ECS-0335765. The authors acknowledge the assistance of Dr David C. Bell (CNS) and Dr Seung-Min Chung (currently at Samsung) for TEM observation.

References

1 R. G. Gordon, *MRS Bull.*, 2000, **25**, 52–57.
2 T. Minami, *Semicond. Sci. Technol.*, 2005, **20**, S35–S44.
3 R. G. Gordon, *J. Non-Cryst. Solids*, 1997, **218**, 81–91.
4 X. Du, Y. Du and S. M. George, *J. Phys. Chem. A*, 2008, **112**, 9211–9219.
5 A. Rosental, A. Tarre, A. Gerst, J. Sundqvist, A. Hårsta, A. Aidla, J. Aarik, V. Sammelselg and T. Uustare, *Sens. Actuators, B*, 2003, **93**, 552–555.
6 A. B. F. Martinson, J. W. Elam, J. Liu, M. J. Pellin, T. J. Marks and J. T. Hupp, *Nano Lett.*, 2008, **8**, 2862–2866.
7 J. B. K. Tennakone, P. K. M. Bandaranayake, G. R. A. Kumara and A. Konno, *Jpn. J. Appl. Phys.*, 2001, **40**, L732.
8 A. Delabie, J. Swerts, S. V. Elshocht, S.-H. Jung, P. I. Raisanen, M. E. Givens, E. J. Shero, J. Peeters, V. Machkaoutsan and J. W. Maes, *J. Electrochem. Soc.*, 2011, **158**, D259–D263.
9 E. J. W. Crossland, M. Kamperman, M. Nedelcu, C. Ducati, U. Wiesner, D. M. Smilgies, G. E. S. Toombes, M. A. Hillmyer, S. Ludwigs, U. Steiner and H. J. Snaith, *Nano Lett.*, 2008, **9**, 2807–2812.
10 C.-Y. Cho and J. H. Moon, *Adv. Mater.*, 2011, **23**, 2971–2975.
11 S. Gubbala, V. Chakrapani, V. Kumar and M. K. Sunkara, *Adv. Funct. Mater.*, 2008, **18**, 2411–2418.
12 J. Heo, A. S. Hock and R. G. Gordon, *Chem. Mater.*, 2010, **22**, 4964–4973.
13 H. B. Profijt, S. E. Potts, M. C. M. van de Sanden and W. M. M. Kessels, *J. Vac. Sci. Technol., A*, 2011, **29**, 050801.
14 S. O. Kucheyev, J. Biener, T. F. Baumann, Y. M. Wang, A. V. Hamza, Z. Li, D. K. Lee and R. G. Gordon, *Langmuir*, 2008, **24**, 943–948.
15 J. Heo, D. Eom, S. Y. Lee, S.-J. Won, S. Park, C. S. Hwang and H. J. Kim, *Chem. Mater.*, 2009, **21**, 4006–4011.
16 J. W. Elam, J. A. Libera, T. H. Huynh, H. Feng and M. J. Pellin, *J. Phys. Chem. C*, 2010, **114**, 17286–17292.
17 J. W. Elam, D. A. Baker, A. J. Hryn, A. B. F. Martinson, M. J. Pellin and J. T. Hupp, *J. Vac. Sci. Technol., A*, 2008, **26**, 244–252.
18 J. W. Elam, D. A. Baker, A. B. F. Martinson, M. J. Pellin and J. T. Hupp, *J. Phys. Chem. C*, 2008, **112**, 1938–1945.
19 S. K. Karuturi, L. Liu, L. T. Su, Y. Zhao, H. J. Fan, X. Ge, S. He and A. T. I. Yoong, *J. Phys. Chem. C*, 2010, **114**, 14843–14848.
20 S.-J. Won, J.-Y. Kim, G.-J. Choi, J. Heo, C. S. Hwang and H. J. Kim, *Chem. Mater.*, 2009, **21**, 4374–4379.
21 J. M. Jensen, A. B. Oelkers, R. Toivola, D. C. Johnson, J. W. Elam and S. M. George, *Chem. Mater.*, 2002, **14**, 2276–2282.
22 M. Batzill and U. Diebold, *Prog. Surf. Sci.*, 2005, **79**, 47–154.

Published on 03 February 2012 on http://pubs.rsc.org | doi:10.1039/C2JM16557K
Downloaded by Harvard University on 22 February 2012

This journal is © The Royal Society of Chemistry 2012

Electronic Supplementary Material (ESI) for Journal of Materials Chemistry
This journal is © The Royal Society of Chemistry 2012

[Supporting Information]

Atomic Layer Deposition of Tin Oxide with Nitric Oxide as an Oxidant Gas

Jaeyeong Heo,[a] Sang Bok Kim[a] and Roy G. Gordon[a,*]

Department of Chemistry and Chemical Biology, Harvard University, Cambridge, Massachusetts 02138 USA

E-mail:gordon@chemistry.harvard.edu

Growth temperature. The thermal stability of the Sn(II) precursor has not been investigated in detail since the early study in combination with 50 wt.% H_2O_2 was focused on low temperature growth lower than 200 ^oC.[1] In order to determine the starting temperature of precursor decomposition, growth conditions without any NO pulse were repeated at three different substrate temperatures of 250, 280, and 310 ^oC. Fig. S1 shows XRF spectra for these samples where characteristic Sn $L_{\alpha1}$ (3.443 keV) and $L_{\beta1}$ (3.662 keV) peaks are monitored. The background spectrum as a control was collected on a SiO_2/Si substrate. It is clearly seen from the Fig. S1 that the spectrum for

250 ^{o}C is almost overlapped with the standard spectrum; however the one for 280 ^{o}C shows small increase in intensity for both peaks, which is a sign of partial decomposition of the precursor. When the temperature is further increased up to 310 ^{o}C, the spectrum obviously shows more intense tin peaks. Based on these observations, it appears that this Sn(II) precursor is stable up to 250 ^{o}C and its decomposition starts at ~280 ^{o}C. If not mentioned otherwise, the film growth and characterization were done on films grown at temperatures of 250 ^{o}C or less.

Optical properties. Fig. S2a shows the optical transmission and reflection spectra of a ~110 nm-thick SnO_2 film deposited at 250 ^{o}C on a quartz substrate. The average transmission in the visible region from 400 to 700 nm was 87.2%, which is comparable to other reports for ALD-grown SnO_2.[1, 2] The Fig. S2b shows a plot appropriate for a direct transition of $(\alpha h\nu)^2$ versus photon energy, where α is the absorption coefficient and $h\nu$ is the incidence photon energy. Linear behavior is found at photon energies over 4.2 eV. The estimated band gap of the SnO_2 film was 4.23-4.27 eV. This band gap is wider than the value ~3.6 observed for undoped SnO_2.[3, 4] This widening is known as the Burstein-Moss shift, which is due to the high carrier concentration in the conduction band.[5]

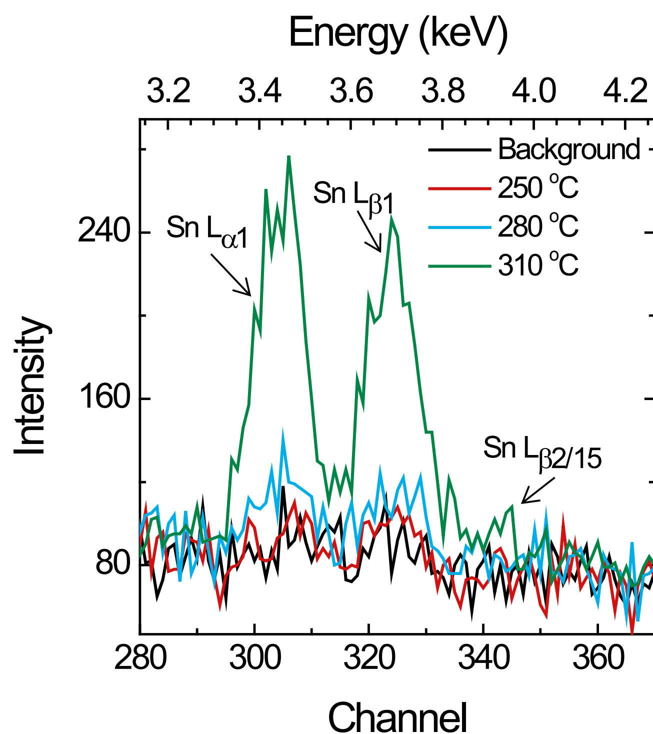

Fig. S1 XRF spectra for samples deposited at various temperatures. The background spectrum was obtained from a SiO_2/Si substrate. Three samples were exposed to Sn precursor vapor (250 cycles) without any oxidant pulse. Increases in the peak intensities of Sn L lines are noted for the 280 and 310 °C samples, which suggests thermal decomposition of the Sn(II) precursor.

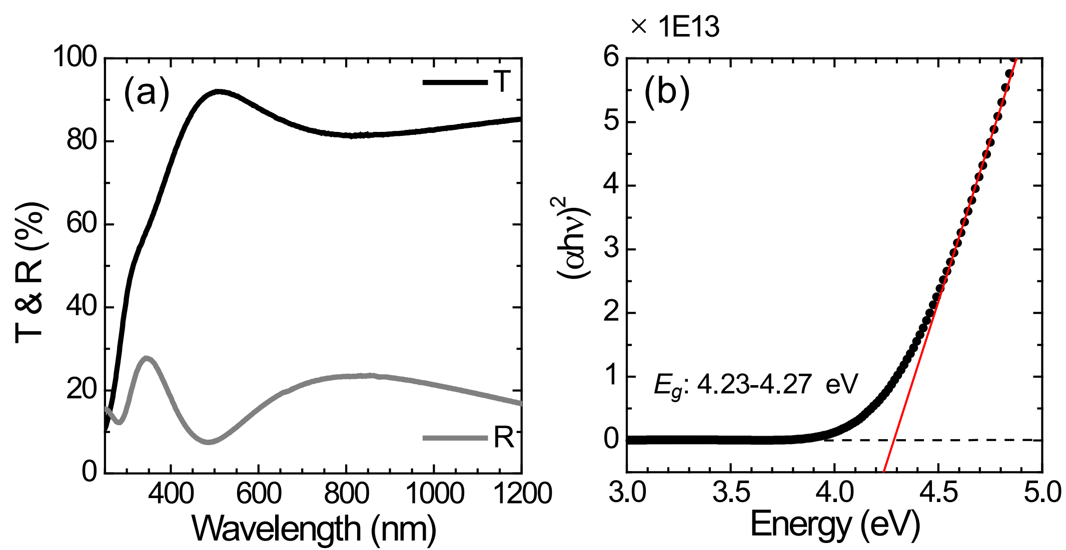

Fig. S2 (a) Transmission and reflection spectra for ~110nm-thick SnO_2 film grown at 250 ^oC. (b) Corresponding direct band gap plot.

This journal is © The Royal Society of Chemistry 2012

References

1. J. Heo, A. S. Hock and R. G. Gordon, *Chem. Mater.*, 2010, **22**, 4964-4973.
2. J. W. Elam, D. A. Baker, A. J. Hryn, A. B. F. Martinson, M. J. Pellin and J. T. Hupp, *J. Vac. Sci. Technol. A*, 2008, **26**, 244-252.
3. R. G. Gordon, *MRS Bull.*, 2000, **25**, 52-57.
4. T. Minami, *Semicond. Sci. Technol.* , 2005, **20**, S35-S44.
5. M. Batzill and U. Diebold, *Prog. Surf. Sci.*, 2005, **79**, 47-154.